JOURNAL OF APPLIED ELECTROCHEMISTRY 18 (1988) 38–42

Evaluation of charge transfer resistance by geometrical extrapolation of the centre of semicircular impedance diagrams

PIERRE R. ROBERGE, RÉJEAN BEAUDOIN

Royal Military College of Canada, Kingston, Ontario, Canada K7K 5L0

Received 8 October 1986; revised 27 May 1987

A simple analysis of impedance diagrams has been performed by using a geometrical technique that determines the centres formed by three successive data points. Such a technique allows monitoring of the corrosion rate of a specimen using as few as three frequencies in the high-frequency part of the diagrams. This greatly reduces the measurement time. Experimental results obtained with copper–nickel alloys are discussed.

1. Introduction

Impedance techniques are finding increasing applications in corrosion research because of the possibility of obtaining information on the chemical mechanisms involved. One main advantage of the a.c. impedance technique is the use of very small signals which do not disturb the sample properties to be measured; a.c. impedance spectroscopy is also unique since it gives access to both the polarization and to the double layer capacitance from the same measurements.

Recording and analysis of a.c. impedance data for corrosion studies, in the case of simple electrochemical reactions that can be represented by an equivalent electrical circuit as shown in Fig. 1, have been described [1]. Hladky *et al.* [2] have presented a graphical method allowing calculation of the charge transfer resistance of an interface. Their technique is only valid for simple systems giving a clear semicircle. Lemaître *et al.* [3] introduced a graphical analysis based on the same tangential technique to estimate the charge transfer resistance in the case of inclined semicircular complex impedance diagrams. For many corroding metals, such as iron in aqueous sulphuric acid, the experimental impedance data cannot be described by semicircles which have their centres on the real axis [4]. The depression of these centres was explained by Cole and Cole [5] on the assumption of a frequency or of a time constant dispersion. This time constant dispersion could also be attributed to inhomogeneities in the electrode surface [2].

The a.c. impedance method is not widely used for corrosion rate monitoring mainly because of the time needed to measure the full impedance diagrams. The purpose of this paper is to present a simple technique that permits approximation of the values of the semicircle diameters by using the high-frequency part of the diagrams. This method of reducing the measurement time has been applied to monitoring the corrosion rate of a copper–nickel alloy under hydrodynamic conditions.

2. Basics of impedance

An electrochemical cell is characterized by the solution impedance, Z_s, which is due to the resistivity of the solution, and by the interfacial impedance, Z_i, which is itself composed of a capacitance, Z_c, arising from the departure of the composition from electroneutrality (electrical double layer) [6] and of a faradaic impedance, Z_f, associated with the charge transfer reaction [7].

Charge transfer resistance, also called polarization resistance (R_p), can be evaluated from the diameter of the semicircles formed by the impedance diagrams [2, 3]. Corrosion rates can then be related to the reciprocal of R_p with the Stearn–Geary low overvoltage approximation of the Butler–Volmer equation.

3. Geometrical extrapolation

The method that has been developed consists of finding the centre of an arc formed by three successive data points on the complex impedance diagram as illustrated in Fig. 2. The experimental points a, b and c, with their corresponding coordinates $((x_1, y_1), (x_2, y_2), (x_3, y_3))$, are linked by the segments ab and bc which have the calculated points (x_4, y_4) and (x_5, y_5) as centres. The slopes of the perpendicular lines to the segments ab and bc are calculated with Equations 1 and 2.

$$P_1 = \frac{y_2 - y_1}{x_2 - x_1} \quad (1a)$$

$$P_2 = \frac{y_3 - y_2}{x_3 - x_2} \quad (1b)$$

$$P_3 = \tan(\text{inv tan } P_1 + 90°) \quad (2a)$$

$$P_4 = \tan(\text{inv tan } P_2 + 90°) \quad (2b)$$

From these slopes, P_3 and P_4, we can find the intercepts y_6 and y_7 (Equation 3) with the Y-axis made by the lines that pass through (x_4, y_4) and (x_5, y_5) respectively.

0021-891X/88 $03.00 + .12

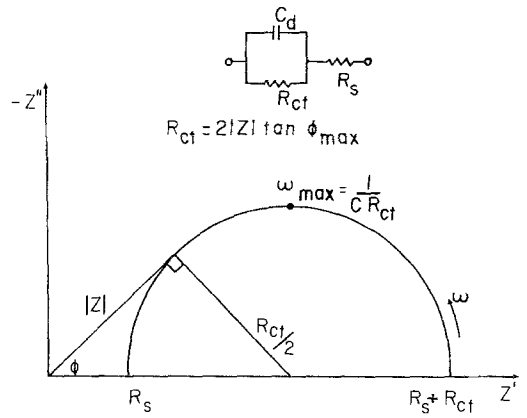

Fig. 1. Theoretical equivalent circuit of a corroding electrode and its corresponding complex plane impedance diagram.

$$y_6 = y_4 - P_3 x_4 \quad (3a)$$

$$y_7 = y_5 - P_4 x_5 \quad (3b)$$

Equation 4 leads to the common point (x_8, y_8) of those two straight lines which is the centre of the semicircle made by the original data points (x_1, y_1), (x_2, y_2) and (x_3, y_3).

$$x_8 = \frac{y_7 - y_6}{P_3 - P_4} \quad (4a)$$

$$y_8 = y_6 + P_3 x_8 \quad (4b)$$

If an impedance diagram had a semicircular shape, slightly depressed as for most reactions, the projected centres would be found in the fourth quadrant, as shown by point a in Fig. 3, with a small dispersion reflecting the precision of the measurements. For a pseudo-inductive loop, the low frequency points would give centres evolving in the fourth, third, second or first quadrant depending on the radius of the loop. In the case of a Warburg component, as shown in Fig. 3, the high-frequency data would have a common centre in the fourth quadrant. This centre would then be displaced as the diffusional component becomes the controlling factor. As the transition between the semicircular shape and the 45° straight line, the extrapolated centre would switch typically from the fourth quadrant to the first and then to the second quadrant; for the straight 45° Warburg component, the projected centre would be far in the second or fourth quadrant depending on the alignment of the points. If an impedance diagram were composed of two successive semicircles, its analysis would give two centres allowing the evaluation of their diameters.

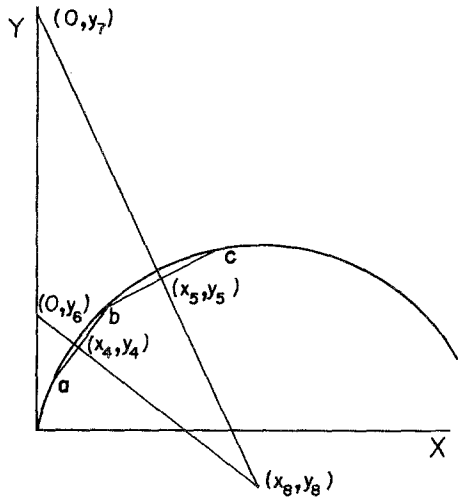

Fig. 2. Schematic representation of the graphical method used to determine the centre of a semicircle.

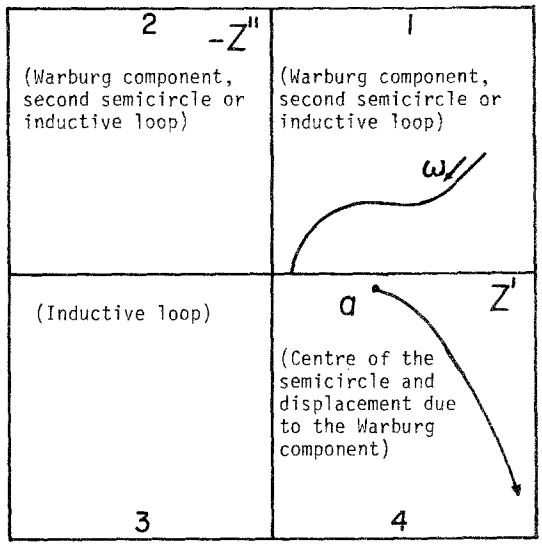

Fig. 3. The distribution of the centres projection for some impedance diagrams showing the most common behaviours.

4. Admittance diagrams

Jonscher [8] has presented impedance and admittance diagrams for different equivalent electrical circuits. Plotting the admittance diagram provides clearer information than plotting the usual impedance diagram. Equation 5 gives the relation between impedance and admittance. (Real part – Z', Y'; imaginary part – Z'', Y''.)

$$\frac{Z'}{Y'} = \frac{Z''}{Y''} = (Z')^2 + (Z'')^2 = \frac{1}{(Y')^2 + (Y'')^2} \quad (5)$$

It can be seen that the high-frequency data of the admittance plot yield an arc extrapolating to $1/R_p$.

If a vectorial subtraction of the solution resistance, R_s, is made, the high-frequency part of the admittance plot becomes controlled by the capacity value, $Y'' = \omega C$. Another technique to obtain the value of the capacity is by plotting Y''/ω versus Y'/ω which gives a straight line with an intercept on the Y-axis (extrapolated from the high-frequency data) that is proportional to the capacity.

5. Experimental details

The alloy used in this study was a 70–30 copper–nickel alloy specifically designed for seawater piping systems. The specimens were machined from a cast sample in cylindrical shapes, of diameter 1.2 cm and height of 2.6 cm, making a total exposed surface of 10 cm^2. The

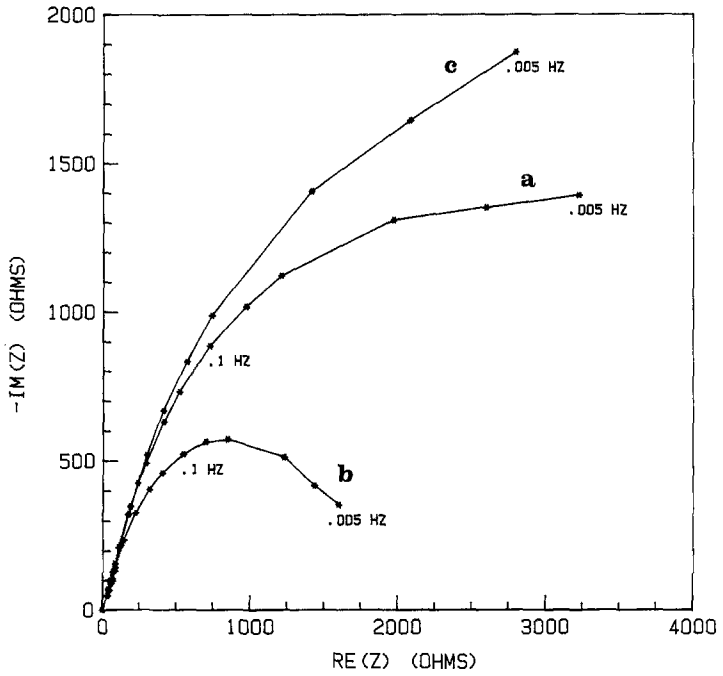

Fig. 4. Impedance diagrams made on a 10-day passivated 70–30 copper–nickel alloy: (a) in a quiescent condition; (b) after 8 h of rotation at 5000 r.p.m.; (c) in a quiescent condition 16 h after the rotation period.

cylindrical specimens were polished to 500 grit, then washed with a good degreasing agent, methylene chloride, with fresh reagent grade acetone and then with doubly distilled water. This pretreatment procedure is similar to the method proposed by Dobb *et al.* [9]. The samples were immersed in saline solution for a period of 10 days. Macdonald *et al.* [10] have shown that the corrosion potential reaches a stable value after 5 days, indicating a steady state in the film formation.

The one-compartment cell was a closed, 2-litre beaker containing 1 litre of electrolyte. The 3% NaCl solution was made up with doubly distilled water and ACS grade NaCl. The cell was left at room temperature (21° C) and purged with air.

The electrochemical impedance measurements were made with an a.c. generator–analyser Solartron model 1250 controlled by a Hewlett–Packard model HP85 microcomputer. The sample was screwed into the rotating assembly (Pine Instrument Company) and the measurements were made without rotation and at 5000 r.p.m.

The hydrodynamic conditions for this cell geometry were characterized by measuring the limiting current of the oxygen reduction reaction at different rotation speeds on a similarly machined pure copper cylinder following a technique originally described by Ponzano *et al.* [11]. A rotation speed of 5000 r.p.m. applied to the cylinders would thus correspond to an average seawater velocity of $3.75\,m\,s^{-1}$ in a tube having a diameter of 2.5 cm.

6. Results and discussion

Fig. 4 shows the impedance diagrams obtained with a 70–30 copper–nickel alloy in three equilibrium con-

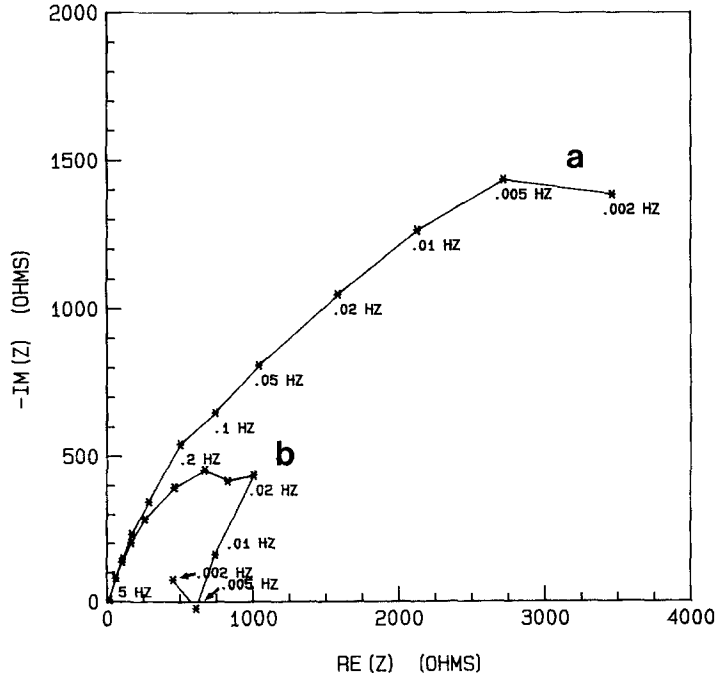

Fig. 5. Impedance diagrams made on a 10-day passivated 70–30 copper–nickel alloy: (a) in a quiescent condition; (b) diagram immediately made when the rotation at 5000 r.p.m. is started.

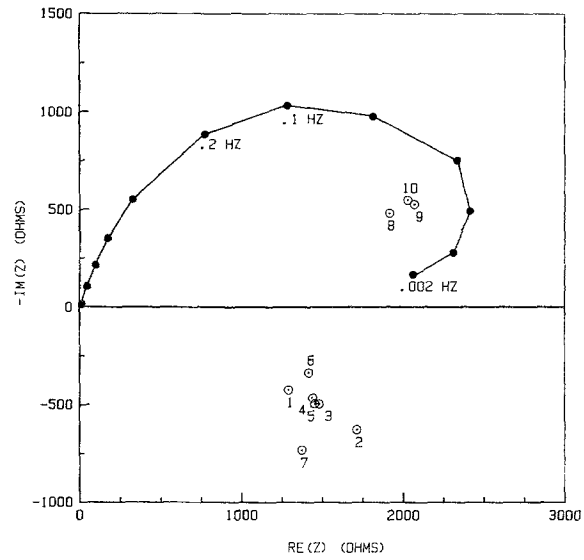

Fig. 6. Impedance diagram made on a 10-day passivated 70–30 copper–nickel alloy after 1 h of rotation at 5000 r.p.m. (●); the extrapolated centres (⊙).

ditions. Curve a is a typical diagram obtained after 10 days in saline solution; curve b was obtained after 8 h at a rotation speed of 5000 r.p.m. If one tries to obtain a complete diagram during the first hours of rotation, the changes are faster than the measurement time, leading to an apparent breakdown (Fig. 5) or a pseudo-inductive loop as shown in Fig. 6. In both these two cases the results cannot be simply analysed and can lead to erroneous conclusions. The example shown in Fig. 6 seems to be a well-developed complex diagram, but a closer examination reveals a good RC behaviour for high frequencies followed by a progressively inductive behaviour toward the lower frequency part of the diagram. This apparent inductive loop is caused by relatively slow changes in the specimen properties, in contrast with the fast changes due to the breakdown of the passivation film visible in Fig. 5.

Table 1. Polarization resistance extrapolated from the admittance diagram and from the centres formed by three points shown in Fig. 7

Curve	*Time (h)*	*Rotation (r.p.m.)*	*Centres ($k\Omega\,cm^{-2}$) (±5%)*	*Admittance ($k\Omega\,cm^{-2}$) (±5%)*
a	0	0	35	37
a[1]	0.25	5000	35	37
b	0.50	5000	22.5	24
c	0.75	5000	19.0	19.0
d	2.5	5000	15.0	15.5
e	5.0	5000	15.5	15.0

(a[1] is superimposed on a)

Curve c in Fig. 4 represents the impedance diagram 16 h after the rotation period. During the reconstitution of the passivation film it would not be possible to explain the full diagram with simple RC models.

Fig. 7 shows the diagrams made with only four frequencies, in the high frequency part (1–0.05 Hz) of the diagram. The projection of centres from those four data points lead to two points. The presence of centres below the real axis is generally attributed to the surface heterogeneity caused by a distribution of the reaction rate with the location on the electrode surface [2, 5, 12]. Such a phenomenon is common with passivated alloys. The measurement time in this case was less than 1 min. Such a short time allows an almost instantaneous evaluation of R_p during the evolution of the phenomena themselves. Table 1 compares some R_p values evaluated from the projection of the centres with the corresponding values calculated from admittance diagrams as a function of time. The agreement between the two types of calculations is within the experimental error.

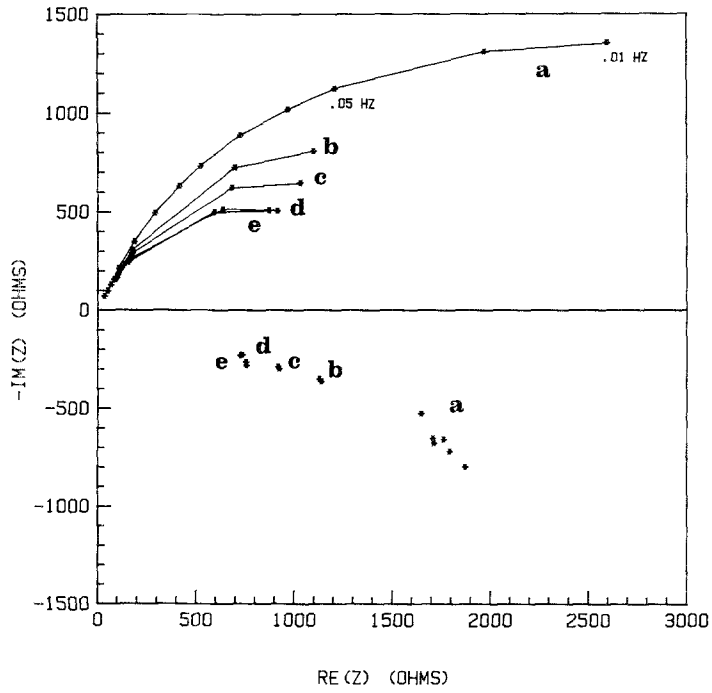

Fig. 7. Evolution of the impedance diagrams and of the projected centres for a 10-day passivated copper–nickel cylinder rotating at 5000 r.p.m.: (a) diagram in quiescent condition; (b), (c), (d) and (e) diagrams made using four high-frequency measurements after 30, 45, 150 and 300 min of rotation of 5000 r.p.m.

7. Conclusion

Determination of R_p from the centre of an arc formed by three appropriate frequencies makes electrochemical impedance a suitable technique for corrosion monitoring by reducing the measurement time. By using this technique it becomes possible to follow the corrosion current (R_p) of a prepassivated alloy under hydrodynamic conditions and especially during fast changes of the impedance.

Acknowledgements

The support of this research by the Defense Research Establishment Atlantic is gratefully acknowledged. We are indebted to Dr R. S. Hollingshead and C. M. Hanham for helpful information concerning the marine applications and behaviours of the copper–nickel alloys, and to Dr M. Sahoo for providing them.

References

[1] F. Mansfeld, *Corrosion* **36** (1981) 301.
[2] K. Hladky, L. M. Callow and J. L. Dawson, *Brit. Corr.* **15** (1980) 20.
[3] L. Lemaître, M. Moors and A. P. Van Peteghem, *J. Appl. Electrochem.* **13** (1983) 803.
[4] I. Epelboin and M. Keddam, *J. Electrochem. Soc.* **117** (1970) 1050.
[5] R. H. Cole and K. S. Cole, *J. Chem. Phys.* **9** (1941) 341.
[6] D. M. Mohilner, in 'Electroanalytical Chemistry', Vol. 1, (edited by A. J. Bard), Marcel Dekker, New York (1966) chap. 4.
[7] M. Sluyters-Rehbach and J. H. Sluyters, in 'Electroanalytical Chemistry', Vol. 4, (edited by A. J. Bard), Marcel Dekker, New York (1970).
[8] A. K. Jonscher, 'Dielectric Relaxation in Solids', Chelsea Dielectrics Press, London (1983).
[9] D. E. Dobb, J. P. Storvick and G. K. Pagenkopf, *Corros. Sci.* **26** (1986) 525.
[10] D. D. Macdonald, B. C. Syrett and S. S. Wing, *Corrosion* **34** (1978) 289.
[11] G. P. Ponzano, M. Bassoli and P. L. Bonora, *Werkit. korros.* **27** (1976) 568.
[12] A. Bonnel, F. Dabosi, C. Deslouis, M. Duprat, M. Keddam and B. Tribollet, *J. Electrochem. Soc.* **130** (1983) 753.